Published in final edited form as:
Cancer Prev Res (Phila). 2014 January ; 7(1): 23–32. doi:10.1158/1940-6207.CAPR-13-0262.

Clinical and biochemical studies support smokeless tobacco's carcinogenic potential in the human oral cavity

Susan R. Mallery[1,2], **Meng Tong**[1], **Gregory C. Michaels**[3], **Amber R. Kiyani**[1], and **Stephen S. Hecht**[4,5]

[1]Division of Oral Maxillofacial Pathology and Radiology, College of Dentistry, The Ohio State University

[2]The Ohio State University Comprehensive Cancer

[3]Division of Oral Maxillofacial Surgery and Anesthesiology, College of Dentistry, The Ohio State University

[4]College of Medicine University of Minnesota

[5]Masonic Cancer Center University of Minnesota

Abstract

In 2007, International Agency for Cancer Research presented compelling evidence that linked smokeless tobacco use to the development of human oral cancer. While these findings imply vigorous local carcinogen metabolism, little is known regarding levels and distribution of Phase I, II and drug egress enzymes in human oral mucosa. In the study presented here, we integrated clinical data, imaging and histopathologic analyses of an oral squamous cell carcinoma that arose at the site of smokeless tobacco quid placement in a patient. Immunoblot and immunohistochemical (IHC) analyses were employed to identify tumor and normal human oral mucosal smokeless tobacco-associated metabolic activation and detoxification enzymes. Human oral epithelium contains every known Phase I enzyme associated with nitrosamine oxidative bioactivation with ~2 fold inter-donor differences in protein levels. Previous studies have confirmed ~3.5 fold inter-donor variations in intraepithelial Phase II enzymes. Unlike the superficially located enzymes in non-replicating esophageal surface epithelium, IHC studies confirmed oral mucosal nitrosamine metabolizing enzymes reside in the basilar and suprabasilar region which notably is the site of ongoing keratinocyte DNA replication. Clearly, variations in product composition, nitrosamine metabolism and exposure duration will modulate clinical outcomes. The data presented here form a coherent picture consistent with the abundant experimental data that links tobacco-specific nitrosamines to human oral cancer.

Keywords

smokeless tobacco; nitrosamines; oral squamous cell carcinoma; nitrosamine metabolism

Corresponding Author: Susan R. Mallery, [1]Division of Oral Maxillofacial Pathology and Radiology, College of Dentistry, 2191B Postle Hall, 305 W12th Ave, The Ohio State University, Columbus OH 43210. Phone: 614-292-5892; FAX: 614-292-9384; mallery.1@osu.edu.

None of the contributing authors have any conflict of interest with the work presented in this paper.

Introduction

In 2007, the International Agency for Research on Cancer (IARC) presented compelling evidence that smokeless tobacco is a human carcinogen and its use is attributable for the development of oral, esophageal and pancreatic cancers [1]. Despite these data, the idea that smokeless tobacco users face a legitimate and heightened risk of developing oral squamous cell carcinoma (OSCC) has not been uniformly accepted among health care providers. OSCCs that developed in smokeless tobacco users were frequently dismissed as attributable to other risk factors such as use of cigarettes and/or alcohol [2, 3].

Despite the clear conclusions of the IARC report, recent epidemiologic literature reviews persist in describing the “harmless nature” of smokeless tobacco [2, 3]. Statements such as “epidemiologic evidence has not shown strong evidence of elevated tobacco-related disease risks with smokeless tobacco use” perpetuate the misconception regarding smokeless tobacco hazards [2]. A significant confounding variable is the dramatic variations-frequently geographic-in the composition of smokeless tobacco products [4]. While Scandinavian cohort studies report data derived from use of the reduced nitrosamine smokeless products common in Northern Europe [4], many of the smokeless tobacco brands that are popular in the U.S. contain appreciably higher nitrosamine levels [5].

With regard to composition, smokeless tobacco is a heterogeneous product that contains nicotine and other tobacco alkaloids in addition to multiple carcinogens including nitrosamines, nitroso-amino acids, polycyclic aromatic hydrocarbons, aldehydes and metals [4]. Notably, smokeless tobacco use results in exposure to 100 to 1000 fold higher nitrosamine levels relative to those obtained via food e.g. cured meat or beverage consumption such as beer [4]. In particular, two smokeless tobacco-associated nitrosamines i.e. N′-nitrosonornicotine (NNN) and 4-(methylnitrosamino)-1-(3-pyridyl)-1-butanone (NNK) are strongly associated with its procarcinogenic effects [1]. In addition, the large product variations in smokeless tobacco e.g. moist long cut, snuff, pouches, snus combined with variations in nitrosamine levels complicates interpretation of epidemiologic studies [4]. Finally, these extensive inter-product differences preclude use of “pouch years” per se as a potential risk indicator of future OSCC development.

The relative risk of developing OSCC from smokeless tobacco use reflects a composite of factors that include product type, duration of usage and intraoral nitrosamine metabolism by surface epithelia. Tobacco-associated nitrosamines can be oxidatively metabolized by a variety of Phase I cytochrome P450 enzymes (P450s) i.e. P450 1A2, P450 2E1, P450 2A6, P450 2A13, and P450 3A4 [6, 7]. Optimally P450-mediated oxidations would reduce nitrosamines’ carcinogenicity as their purpose is detoxification. P450 catalyzed reactions, however, also have the potential to bioactivate nitrosamines to reactive, mutagenic electrophiles [6, 7]. Fortuitously, nitrosamines are also substrates for the Phase II UDP glururonosyl transferase enzymes, which catalyze the addition of glucuronic acid, thereby increasing water solubility and xenobiotic excretion [8, 9]. Unlike their Phase I counterparts, Phase II enzymes primarily function to detoxify xenobiotics [8, 9]. Analogous to other tissues with high metabolic enzyme activities, the distribution of Phase I relative to Phase II enzymes in addition to actual levels of xenobiotic metabolizing enzyme in the mouth will impact the relative risk of developing OSCC during smokeless tobacco use.

Compared to human liver, which has undergone extensive profiling of metabolic enzymes and identification of enzymatic polymorphisms, human oral mucosa has been largely under explored. In earlier studies, our laboratory confirmed the presence of the key polycyclic aromatic hydrocarbon metabolizing enzymes P450s 1A1, 1A2 and 1B1 in human oral tissues [10]. More recently, we demonstrated that human oral mucosa contains a rich supply

of Phase I, II and III (drug egress) enzymes which are associated with anthocyanin metabolism [11]. This recent study also revealed appreciable (over 300 fold) variations in levels of key metabolic enzymes; findings that are consistent with the recognized extensive inter-individual heterogeneity in human metabolic enzymes [11]. Additionally, nitrosamine metabolism is further complicated by genetic polymorphisms which render some isoforms totally or partially inactive [12, 13]. Relevant polymorphisms are present in the P450 2A6 which has the potential to bioactivate nitrosamine procarcinogens [12].

Essential aspects such as oral mucosal metabolic enzyme profiles and inter-donor enzyme heterogeneity responsible for nitrosamine-mediated oral carcinogenesis remain unknown. The purpose of this study was therefore to present coordinated clinical data and investigations of human oral cavity nitrosamine relevant enzymes with integration of published animal model data to depict how smokeless tobacco use initiates human OSCC development.

Materials and Methods

Participation of human subjects

Human subjects participation in these studies was in accordance with The Ohio State University Institutional Review Board approval and followed the tenets of the Declaration of Helsinki 1964.

Evaluation of Phase I cytochrome P450 enzymes (P450s) in human oral mucosa by immunoblot analyses

Eleven cryopreserved samples of normal oral mucosal tissue lysates were obtained from our previous study [11]. Human liver tissue extract (Imgenex, San Diego, CA) was employed as a positive control. Western blots were conducted by using the iBlot system and 4%-12% precast NuPage Bis-Tris gels (Invitrogen, Grand Island, NY). As the human liver tissue was expected to contain markedly higher levels of evaluated enzymes than normal human oral mucosal tissues, only one third of total liver tissue extract (10μg/lane) was loaded relative to the oral mucosal tissue lysates (30μg/lane). The involved primary antibodies and their working dilutions are: P450 1A2 (1:200, mouse monoclonal, Santa Cruz Biotechnology, Santa Cruz, CA), P450 2A6 (1:200, mouse monoclonal, Santa Cruz Biotechnology, Santa Cruz, CA), P450 2A13 (1:100, rabbit polyclonal, AbCam, Cambridge, MA), P450 2E1 (1:200, Santa Cruz Biotechnology, Santa Cruz, CA), P450 3A4 (1:200, mouse monoclonal, Santa Cruz Biotechnology, Santa Cruz, CA). β-actin (1:5000, Santa Cruz Biotechnology, Santa Cruz, CA) was used as a loading control. Proteins were visualized using ECL Plus Western Blotting Detection system (GE Healthcare/Amersham, Piscataway, NJ) followed by exposure to Kodak films (Kodak, Rochester, NY) and densitometry analyses (Kodak 1D3 image analysis software (Kodak, Rochester, NY). Results were normalized relative to endogenous β-actin levels.

Immunohistochemical staining

The smokeless tobacco-associated OSCC tumor tissue and seven normal oral mucosal specimens were sectioned for immunohistochemical staining to confirm the presence of nitrosamine-related metabolic enzymes and to evaluate their distribution and localization. The normal mucosal specimens were obtained from matching tissue sites as the OSCC tumor i.e. buccal vestibule and mandibular gingiva. The primary antibodies and their working dilutions are as follows: UGT1A (1:200, rabbit polyclonal, Santa Cruz Biotechnology, Santa Cruz, CA), BCRP (1:20, mouse monoclonal, Abcam, Cambridge, MA), UDP-Glu-DH (1:50, mouse monoclonal, Santa Cruz Biotechnology, Santa Cruz, CA), MRP1 (1:50, mouse monoclonal, Santa Cruz Biotechnology, Santa Cruz, CA), P450 1A2

(1:50, mouse monoclonal, Santa Cruz Biotechnology, Santa Cruz, CA), P450 2A6 (1:50, mouse monoclonal, Abcam, Cambridge, MA), P450 2A13 (1:50, rabbit polyclonal, AbCam, Cambridge, MA), P450 2E1 (1:50, Santa Cruz Biotechnology, Santa Cruz, CA), P450 3A4 (1:50, mouse monoclonal, Santa Cruz Biotechnology, Santa Cruz, CA). Blocking buffer was used in place of primary antibody to serve as the negative control. Commercially available human liver tissue slides served as the positive control (Imgenex, San Diego, CA). Sections were incubated with their respective biotinylated secondary antibody (1:200, Vector Laboratories, Burlingame, CA) followed by application of Vectastain ABC reagent (Vector Laboratories). Immunoreactions were visualized using the DAB substrate, followed by hematoxylin counterstaining. Images were captured using a Nikon DS-Fi-1 high-resolution digital camera and analyzed using Image-Pro Plus 6.2 software (Media Cybernetics, Bethesda, MD, USA).

Image Analysis

Image analyses were conducted using the ImagePro Plus 6.2 software (Media Cybernetics, Bethesda, MD) in order to provide a more quantitative assessment of immunohistochemical staining. Staining intensity thresholds were established based upon areas of strong, medium, weak and no immunoreactivity in stained tissues. The percentage areas of strong, medium, weak and no staining regions were then automatically calculated based on the selected intensity thresholds. The H-Score was employed in this study for evaluation of the enzyme expression extent in both smokeless tobacco associated SCC and normal oral epithelium. The H-Score was calculated following the modified formula: H-Score = 3x strong staining area% + 2x medium staining area% + 1x weak staining area% [14, 15]. The H-Score range is from 0 to 300, where the maximum value “300” stands for 100% cells presenting strong staining, and “0” stands for no staining.

Results

Clinical case information

A 51 year old Caucasian male was referred to a local oral and maxillofacial surgeon for management of an intraoral growth. His presenting chief complaint was “sore in lower jaw and loose teeth”. The patient’s previous medical history was unremarkable. He did, however, report a 10 year history of placement of Fine Cut Grizzly moist snuff with the duration from minutes to several hours daily. Notably, per patient history, he recalled occasionally falling asleep with smokeless tobacco in his mouth, resulting in 8 plus hours of tobacco-mucosal contact. The tobacco placement site (left posterior mandible) matched the site of a lesion in his mandibular vestibule (See Fig. 1A.). Other aspects of his social history were notable in that he reported never smoking cigarettes and had modest (1 to 2 drinks per week) alcohol use. Such self-reported information, however, is entirely based on the patient’s ability for accurate recall.

Extraoral examination was unremarkable; all head and neck lymph nodes were non-palpable and non-tender and no facial asymmetry was noted. Intraorally, an exophytic, focally ulcerated 3.5 by 3.0 cm tumor was observed that extended from the buccal gingiva of the second mandibular premolar to the distal aspect of the second mandibular molar and also involved the associated buccal vestibule (Fig. 1A) and corresponded to the site where smokeless tobacco was placed. The mandibular second molar was extremely mobile. 3D Cone Beam imaging (iCAT) demonstrated complete erosion of the buccal plate associated with the left second mandibular molar with partial erosion of the distal aspect of the buccal plate of the mandibular first molar (Fig. 1B). Also apparent from these imaging studies was the extensive inter-radicular bone loss that was restricted to these two teeth (Fig. 1C). An

incisional biopsy was taken of the tumor tissue which was then submitted to Oral Pathology Consultants at Ohio State University College of Dentistry for histopathologic evaluation.

Microscopic evaluation revealed that the tumor tissue arose from a dysplastic surface oral epithelium. The carcinoma demonstrated an infiltrative growth pattern, cellular and nuclear pleomorphism, a high mitotic index, and production of abundant keratin (Fig. 1D). A moderate to heavy infiltrate of host chronic inflammatory cells were observed in response to the tumor tissue. This lesion was microscopically diagnosed as a well-differentiated squamous cell carcinoma and the patient was referred to an otolaryngologist for tumor resection.

The OSCC surgical procedures were extensive and entailed a tracheostomy, modified left neck dissection, composite resection including hemimandibulectomy combined with a floor of mouth resection and partial glossectomy, and wide resection of buccal mucosa. Surgical site reconstruction entailed use of a fibula osseous-cutaneous free flap with vascular anastomoses in conjunction with mandibular plate stabilization and complex vetibuloplasty. Despite the skill of the attending surgeon, this patient is experiencing significant morbidities including major esthetic issues as well as functional speech and swallowing problems. As of September 2013, approximately ten months post-surgery) the patient remains free of tumor and is being monitored by close clinical follow-up.

Smokeless tobacco-associated OSCC tumor tissue possesses all enzymes necessary for metabolism of tobacco-associated nitrosamines

As is apparent in Figs. 2A and 2B, both the dysplastic overlying surface epithelia and the locally infiltrative OSCC tumor nests demonstrate intracytoplasmic staining for the P450s associated with nitrosamine bioactivation (Figs. 2A and 2B). In addition, P450 enzymes are predominantly located in the epithelium, with negligible staining noted in the connective tissue stroma. P450s 3A4, 2A13 and 1A2 showed the most intense staining, with modest levels observed for P450 2A6 and light staining for P450 2E1. Consistent with our previous data [11], expression of UGT 1A isoforms, Phase III efflux pump (MRP1 and BCRP) and an enzyme that could contribute to local enteric recycling (UDP Glu-DH) expression are also observed in the surface epithelium. Overall, relative to clinically and histologically normal oral epithelia, the tumor IHC results showed more intense and/or more extensive staining for all of the evaluated metabolic enzymes with the exception of P450 2A13 and 3A4. Comparable staining between tumor and dysplastic epithelium for these two P450s were noted (Table I).

Clinically and histologically normal human oral mucosa also contain nitrosamine-metabolizing P450 enzymes; with appreciable inter-donor variations apparent

Clinical and histologically normal human oral mucosa contains all five P450 enzymes that are associated with Phase I nitrosamine metabolism (Figs. 3A and 3B). Beta-actin normalized protein levels reveal approximately two fold inter-donor variations in levels of all P450 enzymes evaluated. In addition, P450s 1A2, 2A6 and 3A4 are present at higher levels relative to P450s 2E1 and 2A13 (Figs. 3A and 3B). Relative to P450 levels contained in human liver, oral mucosal enzymes levels are appreciably lower with oral mucosal P450 2A13 and P450 3A4 representing the highest and lowest, respectively (Table II, Fig. 3).

Nitrosamine-metabolizing enzymes are distributed within the oral epithelia

Consistent with our previous metabolic profiling data [11] and current results generated from the OSCC tumor tissue, nitrosamine metabolizing P450s are primarily distributed in the surface epithelia with appreciably lower levels noted in the stroma and infiltrating inflammatory cells (Figs. 4A and 4B). Furthermore, P450 enzymes' intraepithelial

expression was often highest in the basal and peribasilar epithelial cells, with staining frequently extending into the superficial spinous layers. Notably, the outermost differentiated keratinocytes including the overlying keratin were devoid of any IHC staining (Figs. 4A and 4B). Overall, P450 enzymes IHC levels in normal epithelium were either comparable (P450s 2A13, 3A4) or lower (P450s 1A2, 2A6, 2E1) relative to OSCC tumor tissues (Figs. 3 & 4, Table II).

Discussion

The clinical case conditions presented in this paper approach a near “perfect storm” scenario for development of a smokeless tobacco-mediated oral cancer. Our patient used a smokeless tobacco product with remarkably high nitrosamine content, had a history of sustained product usage at a specific placement site, and his dysplastic oral epithelium and OSCC tumor tissues contained every P450 enzyme associated with oxidative metabolism of nitrosamine in tobacco. Notably, the cytochrome P450 enzymes identified in this study can metabolize a wide variety of compounds including endogenous substrates e.g. eiconsanoids, and xenobiotic carcinogens such as polycyclic hydrocarbons and their diols and vinyl halides and dihaloaklanes [16, 17]. Although UGT 1A enzymes were also present in his tissues, the expanse of P450 enzymes present suggests the prospect for higher levels of oxidatively bioactivated metabolites relative to detoxified nitrosamines.

Smokeless tobacco products vary appreciably in nitrosamine content [1]. For example there is a wide range in the respective levels of the two most procarcinogenic nitrosamines i.e. NNN and NNK in smokeless products currently popular in the U.S. [5]. The product used by the patient presented in this study, the Reynolds American Inc. (RAI) product, Grizzly moist snuff, contains high levels of NNN and NNK which are nearly two-fold higher relative than the next closest high nitrosamine product, Copenhagen snuff, and 5 to 8 fold greater than Camel and Marlboro snus [5]. As manifest by the low levels of nitrosamines in snus products, nitrosamine-reducing technology such as pasteurization is currently available to tobacco companies. Given that nitrosamines are now universally accepted as the most carcinogenic smokeless tobacco constituent, retention of such high levels of NNN and NNK in RAI’s Grizzly-is at best worrisome and has the potential to be considered negligent [5].

Collectively, oral and esophageal mucosal tissues comprise the upper extent of the human digestive system. Relative to human oral mucosa, however, human esophageal nitrosamine metabolism has been more extensively investigated [18, 19]. Studies by Smith et al. provided insights regarding nitrosamine relevant P450 enzymes present in human esophagus i.e. P450 3A4 and 2E1 while reporting the absence of 2A6 [18]. In addition, these investigations demonstrated that esophageal P450 levels were appreciably lower relative to human liver [18]. Geographic-specific variations, which imply a compensatory gain of function, were detected in esophageal Phase II enzyme activities in samples from China where nitrosamine exposure is thought to be higher relative to Europe and North America [18]. Additional investigations by Hughes et al. confirmed the presence of mRNAs for P450s 1A2, 3A4, 2C9 and 2E1 in human esophageal tissues [19]. This apparent discrepancy between the findings of Smith and Hughes may reflect negligible P450 3A4 protein (Smith) with higher amounts of the mRNA transcript (Hughes) [18, 19]. Furthermore, P450 enzymes localization in esophageal surface epithelium was restricted to suprabasilar levels in non-diseased mucosa, but extended to basal layer cells in Barrett esophagitis [19]. In contrast to esophageal epithelium, human oral mucosa displays some distinct differences. Our data confirm that human oral mucosa contains five enzymes (P450s 1A2, 2A6, 2A13, 2E1, 3A4). Furthermore, our complimentary immunoblots and corresponding tissue IHC analyses confirmed that nitrosamine metabolizing enzymes are predominantly located in the surface oral epithelia, with highest distribution in the basilar third. Notably, both 2A6 and 2A13

which can bioactivate NNN and NNK are present [20, 21]. Furthermore, while esophageal nitrosamine metabolizing P450 enzymes in normal esophagus are located in the more superficial spinous layers, in human oral epithelia these P450s-including 2A6 and 2A13 are distributed in microsomes contained in the cytosol of basal and lower level spinous layer keratinocytes. Consistent with stratified squamous epithelium distributed elsewhere in the body, DNA replication and cell division occurs in the basal layer. In contrast, spinous layer keratinocytes, which have begun the transition to terminal differentiation, no longer replicate DNA in histologically normal epithelia. This generation of P450-activated nitrosamine electrophiles in proximity to replicating basal layer keratinocytes and associated transient amplifying cells' DNA could greatly contribute to the probability of mutations in oral epithelia.

Nicotine, which is the addiction-inducing component in smokeless tobacco, is not itself a carcinogen. Each dip of nicotine-delivering smokeless tobacco, however, exposes the user to a mixture of carcinogens including tobacco-specific nitrosamines such as NNN and NNK, nitrosamino acids, volatile nitrosamines, polycyclic aromatic hydrocarbons, aldehydes, and certain metals [1]. The tobacco-specific nitrosamine NNN is arguably the most important carcinogen in smokeless tobacco. All smokeless tobacco products contain NNN, generally in the range of 1 – 10 μg/g of tobacco, amounts which are far higher than similar carcinogens in other consumer products (10 μg of NNN is 56 nmol, or about 34 quadrillion molecules) [1]. A typical smokeless tobacco user will expose him or herself to about 31 μg per day of NNN [22, 23]. Compatible with ongoing nitrosamine metabolism, all smokeless tobacco users release NNN as well as NNAL, a metabolite of NNK, in their saliva and urine [1]. Smokeless tobacco mediated oral cancers most commonly arise at the site of quid placement. Because saliva bathes the oral cavity, salivary-transported NNN and NNAL also present the potential for field carcinogenesis. At the systemic level, amounts of NNN and NNAL in the urine of smokeless tobacco users are somewhat higher than in smokers [24]. Notably, these nitrosamines are not found in the urine of non-tobacco users unless they are exposed to secondhand smoke.

With regard to the mechanisms of smokeless tobacco mediated chemical carcinogenesis, the primary culprit, NNN, exists in left- and right-handed (enantiomeric) forms. The left-handed form, known as (*S*)-NNN, is the predominant form in all smokeless tobacco products [25] and is well established as a powerful carcinogen for the rat esophagus and oral mucosa [26, 27]. A recent study that involved treatment of 20 rats with 14 ppm of (*S*)-NNN in their drinking water resulted in a 100% incidence of oral cavity tumors in all treated rats [28]. Collectively, 89 oral cavity tumors were formed. The rats treated with (S)-NNN developed a spectrum of oral lesions that included the neoplasm squamous papilloma (13 on tongue, 11 oral mucosa, 10 soft palate, 11 epiglottis, 11 pharynx), the premalignant epithelial lesion atypical hyperplasia (15 tongue, 16 oral mucosa, 13 soft palate, 16 epiglottis, 18 pharynx) and the overtly malignant squamous cell carcinoma (2 tongue, 1 oral mucosa, 1 soft palate, 1 epiglottis, 1 pharynx). Contingent upon the extent of histologic atypia and proliferation indices, the lesions classified as squamous papilloma may also represent a premalignant precursor and ultimately transition to papillary or verrucous squamous cell carcinoma [28]. Furthermore, treated rat tumors extended throughout the entire oropharynx in contact with S-NNN including tongue, floor of mouth, soft palate and pharynx [28]. Notably, the patient's levels of total NN exposure (estimated 113.5 mg total over 10 years, assuming a 31 μg/day) compare favorably to the estimated total dose of 123 mg per rat over a span of 17 months [28]. It is important, however, to consider several factors in this daily NNN exposure was most likely higher [5]. Also the patient applied smokeless tobacco to the same site for a period of ten years. In contrast, the NNN administered to the treated rats was incorporated in water which perfused throughout the oral cavity and was not retained at a specific location [28]. A final aspect is the carcinogenic time frame. Due to the shorter life span of rats and

the need to induce tumors in an expeditious fashion, the rats were treated with a high dose (14 ± 2 ppm) at the onset of the experiment [28] whereas the patient had a ten year history of smokeless tobacco use.

The importance of tobacco metabolism in oral carcinogenesis was underscored in a recent study that employed an intact immune system murine model [29]. Topical intraoral application of the "ultimate tobacco carcinogenic metabolite" i.e. the dibenzo[*a*,*l*]pyrene metabolite dibenz[*a*,*l*]pyrene diol epoxide, induced oral squamous cell carcinomas with similar mutation profiles as noted in human OSCCs such as p53 [30]. In contrast, tumors attributable to topical application of the parent compound benzo[*a*]pyrene did not demonstrate the same human-relevant mutations [29, 30]. Although smokeless tobacco is thought to only contain trace amounts of dibenzo[*a*,*l*]pyrene [28], metabolic bioactivation to the ultimate tobacco carcinogen could impact clinical outcome.

This study provides the clinical and biochemical information necessary to depict how smokeless tobacco products can initiate human OSCC. Importantly, this study also demonstrates coherence between clinical and experimental findings in humans and rats. Similar to carcinogen metabolism at other tissues, the ultimate determinants of carcinogenesis reflect the nature of carcinogen, exposure dose and the product composition and levels and distribution of target tissue metabolic enzymes. An important consideration is the preliminary nature of these studies. Additional investigations, which include increased patient numbers, use of different smokeless tobacco products, and additional intra and inter-patient Phase I-Phase II enzyme comparisons, are planned to reinforce these observations. Finally, while persons with a proportionately higher Phase II relative to Phase I intraoral enzyme functions may enjoy a relatively reduced risk of OSCC development, the better choice is to refrain from any form of tobacco use.

Acknowledgments

The authors thank Mary Lloyd and Mary Marin for their expertise in preparation and sectioning of the histologic sections.

Grant Support: This work was supported by NIH grants R01 CA129609 and R01 CA171329.

References

1. International Agency for Research on Cancer. IARC Monographs on the Evaluation of Carcinogenic Risks to Humans. Vol. 89. Lyon: IARC; 2007. Smokeless tobacco and tobacco-specific nitrosamines; p. 41-583.
2. Colilla SA. An epidemiologic review of smokeless tobacco health effects and harm reduction potential. Regul Toxicol Pharmacol. 2010; 56:197–211. [PubMed: 19796662]
3. Lee PN. Summary of the epidemiological evidence relating snus to health. Regul Toxicol Pharmacol. 2011; 59:197–214. [PubMed: 21163315]
4. Boffetta P, Hecht SS, Gray N, Gupta P, Straif K. Smokeless tobacco and cancer. Lancet Oncol. 2008; 9:667–75. [PubMed: 18598931]
5. Hecht SS, Stepanov I, Hatsukami DK. Major tobacco companies have technology to reduce carcinogen levels but do not apply it to popular smokeless tobacco products. Tob Control. 2011; 20:443. [PubMed: 20930058]
6. Kamataki T, Fujita K, Nakayama K, Yamazaki Y, Miyamoto M, Ariyoshi N. Role of human cytochrome P450 (P450) in the metabolic activation of nitrosamine derivatives: application of genetically engineered Salmonella expressing human P450. Drug Metab Rev. 2002; 34:667–76. [PubMed: 12214673]

7. Yamazaki H, Inui Y, Yun CH, Guengerich FP, Shimada T. Cytochrome P450 2E1 and 2A6 enzymes as major catalysts for metabolic activation of N-nitrosodialkylamines and tobacco-related nitrosamines in human liver microsomes. Carcinogenesis. 1992; 13:1789–94. [PubMed: 1423839]
8. Ren Q, Murphy SE, Zheng Z, Lazarus P. O-Glucuronidation of the lung carcinogen4-(methylnitrosamino)-1-(3-pyridyl)-1-butanol (NNAL) by human UDP-glucuronosyltransferases 2B7 and 1A9. Drug Metab Dispos. 2000; 28:1352–60. [PubMed: 11038164]
9. Wiener D, Doerge DR, Fang JL, Upadhyaya P, Lazarus P. Characterization of N-glucuronidation of the lung carcinogen 4-(methylnitrosamino)-1-(3-pyridyl)-1-butanol (NNAL) in human liver: importance of UDP-glucuronosyltransferase 1A4. Drug Metab Dispos. 2004; 32:72–9. [PubMed: 14709623]
10. Rinaldi AL, Morse MA, Fields HW, Rothas DA, Pei P, Rodrigo KA, et al. Curcumin activates the aryl hydrocarbon receptor yet significantly inhibits (−)-benzo(a)pyrene-7R-trans-7,8-dihydrodiol bioactivation in oral squamous cell carcinoma cells and oral mucosa. Cancer Res. 2002; 62:5451–6. [PubMed: 12359752]
11. Mallery SR, Budendorf DE, Larsen MP, Pei P, Tong M, Holpuch AS, et al. Effects of human oral mucosal tissue, saliva, and oral microflora on intraoral metabolism and bioactivation of black raspberry anthocyanins. Cancer Prev Res. 2011; 4:1209–21.
12. Wang S-L, He X-Y, Shen J, Wang J-S, Hong J-Y. The Missense Genetic Polymorphisms of Human CYP2A13: Functional Significance in Carcinogen Activation and Identification of a Null Allelic Variant. Toxicol Sci. 2006; 94:38–45. [PubMed: 16917071]
13. Di YM, Chow VD, Yang LP, Zhou SF. Structure, function, regulation and polymorphism of human cytochrome P450 2A6. Curr Drug Metab. 2009; 10:754–80. [PubMed: 19702528]
14. Detre S, Saccani Jotti G, Dowsett M. A “quickscore” method for immunohistochemical semiquantitation: validation for oestrogen receptor in breast carcinomas. J Clin Pathol. 1995; 48:876–8. [PubMed: 7490328]
15. Rizzardi AE, Johnson AT, Vogel RI, Pambuccian SE, Henriksen J, Skubitz AP, et al. Quantitative comparison of immunohistochemical staining measured by digital image analysis versus pathologist visual scoring. Diagn Pathol. 2012; 7:42. [PubMed: 22515559]
16. Guengerich FP. Metabolism of chemical carcinogens. Carcinogenesis. 2000; 21:345–51. [PubMed: 10688854]
17. Nebert DW, Dalton TP. The role of cytochrome P450 enzymes in endogenous signalling pathways and environmental carcinogenesis. Nat Rev Cancer. 2006; 6:947–60. [PubMed: 17128211]
18. Smith TJ, Liao A, Wang Li-D, Yang G-yu, Starcic S, Philbert AM, et al. Characterization of xenobiotic-metabolizing enzymes and nitrosamine metabolism in the human esophagus. Carcinogenesis. 1998; 19:667–72. [PubMed: 9600353]
19. Hughes SJ, Morse MA, Weghorst CM, Kim H, Watkins PB, Guengerich FP, et al. Cytochromes P450 are expressed in proliferating cells in Barrett’s metaplasia. Neoplasia. 1999; 1:145–53. [PubMed: 10933049]
20. Wong HL, Murphy SE, Hecht SS. Cytochrome P450 2A-Catalyzed Metabolic Activation of Structurally Similar Carcinogenic Nitrosamines: N′-Nitrosonornicotine Enantiomers, N-Nitrosopiperidine and N-Nitrosopyrrolidine. Chem Res Toxicol. 2005; 18:61–9. [PubMed: 15651850]
21. Jalas JR, Hecht SS, Murphy SE. Cytochrome P450 Enzymes as Catalysts of Metabolism of 4-(Methylnitrosoamino)-1(3-pyridyl)-1-butanone, a Tobacco Specific Carcinogen. 2005; 18:95–110.
22. Hecht SS, Carmella SG, Edmonds A, Murphy SE, Stepanov I, Luo X, et al. Exposure to nicotine and a tobacco-specific carcinogen increase with duration of use of smokeless tobacco. Tob Control. 2007; 17:128–31. [PubMed: 18375734]
23. Hecht SS, Carmella SG, Stepanov I, Jensen J, Anderson A, Hatsukami DK. Metabolism of the tobacco-specific carcinogen 4-(methylnitrosamino)-1-(3-pyridyl)-1-butanone to its biomarker total NNAL in smokeless tobacco users. Cancer Epidemiol Biomarkers Prev. 2008; 17:732–5. [PubMed: 18349296]
24. Hecht SS, Carmella SG, Murphy SE, Riley WT, Le C, Luo X, et al. Similar exposure to a tobacco-specific carcinogen in smokeless tobacco users and cigarette smokers. Cancer Epidemiol Biomarkers Prev. 2007; 16:1567–72. [PubMed: 17684130]

25. Stepanov I, Yershova K, Carmella S, Upadhyaya P, Hecht SS. Levels of (S)-N′-nitrosonornicotine in U.S. tobacco products. Nicotine Tob Res. 2013; 15:1305–10. [PubMed: 23212437]

26. Lao Y, Yu N, Kassie F, Villalta PW, Hecht SS. Analysis of pyridyloxobutyl DNA adducts in F344 rats chronically treated with (R)- and (S)-N′-nitrosonornicotine. Chem Res Toxicol. 2007; 20:246–56. [PubMed: 17305408]

27. Zhang S, Wang M, Villalta PW, Lindgren BR, Lao Y, Hecht SS. Quantitation of pyridyloxobutyl DNA adducts in nasal and oral mucosa of rats treated chronically with enantiomers of N′-nitrosonornicotine. Chem Res Toxicol. 2009; 22:949–56. [PubMed: 19405515]

28. Balbo S, James-Yi S, Johnson CS, O'Sullivan MG, Stepanov I, Want M, et al. (S)-N′-Nitrosonornicotine, a constituent of smokeless tobacco, is a powerful oral cavity carcinogen in rats. Carcinogenesis. 2013; 34:2178–83. [PubMed: 23671129]

29. Guttenplan JB, Kosinska W, Zhao A-L, Chen K-M, Aliaga C, DelTondo J, et al. Mutagenesis and carcinogenesis induced by dibenzo[a,l]pyrene in the mouse oral cavity: a potential new model for oral cancer. Int J Cancer. 2012; 130:2783–90. [PubMed: 21815141]

30. Chen KM, Guttenplan JB, Zhang SM, Aliaga C, Cooper TK, Sun YW, et al. Mechanisms of oral carcinogenesis induced by dibenzo[a,l]pyrene: an environmental pollutant and a tobacco smoke constituent. Int J Cancer. 2013; 133:1300–9. [PubMed: 23483552]

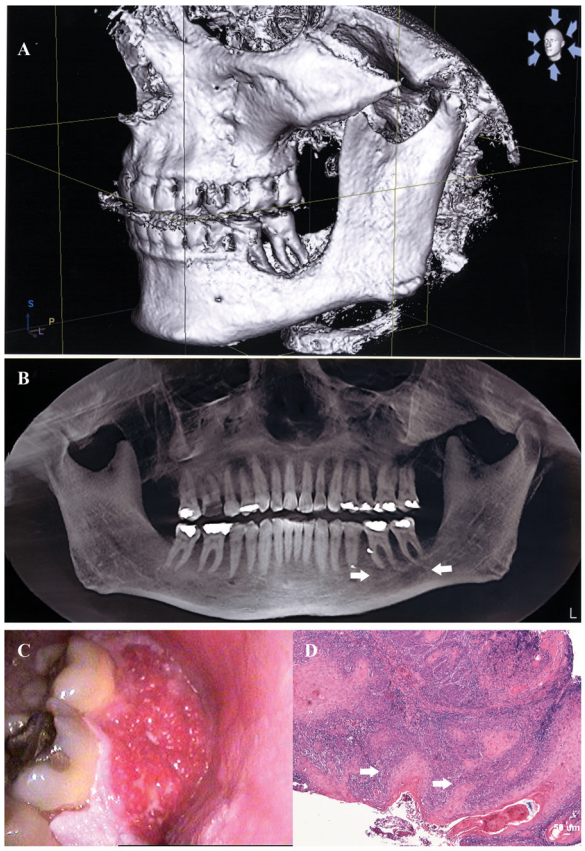

Figure 1.

Fig. 1A is a three dimensional iCAT image of the buccal aspect of the patient's left body of the mandible. Readily apparent is the marked bone destruction associated with his second and first mandibular molars-which corresponds to the placement site for the smokeless tobacco quid. Fig. 1B is a panoramic view of the patient's iCAT image which reveals pronounced inter-radicular bone loss (arrows) which is restricted to the smokeless tobacco placement site. Fig. 1C is a clinical photograph of the patient's OSCC tumor. The surface is micronodular and focally ulcerated as indicated by areas of fibrin deposition. The erythematous color corresponds to both the highly angiogenic nature and the presence of numerous host chronic inflammatory cells. The OSCC tumor histopathology (4x image scale) is depicted in Fig. 1D. Tumor cells arise from an overlying hyperkeratotic dysplastic surface epithelium (arrow). An intense host chronic inflammatory cell infiltrate (small blue cell infiltrate) is noted in association with the dysplastic epithelium and OSCC tumor nests.

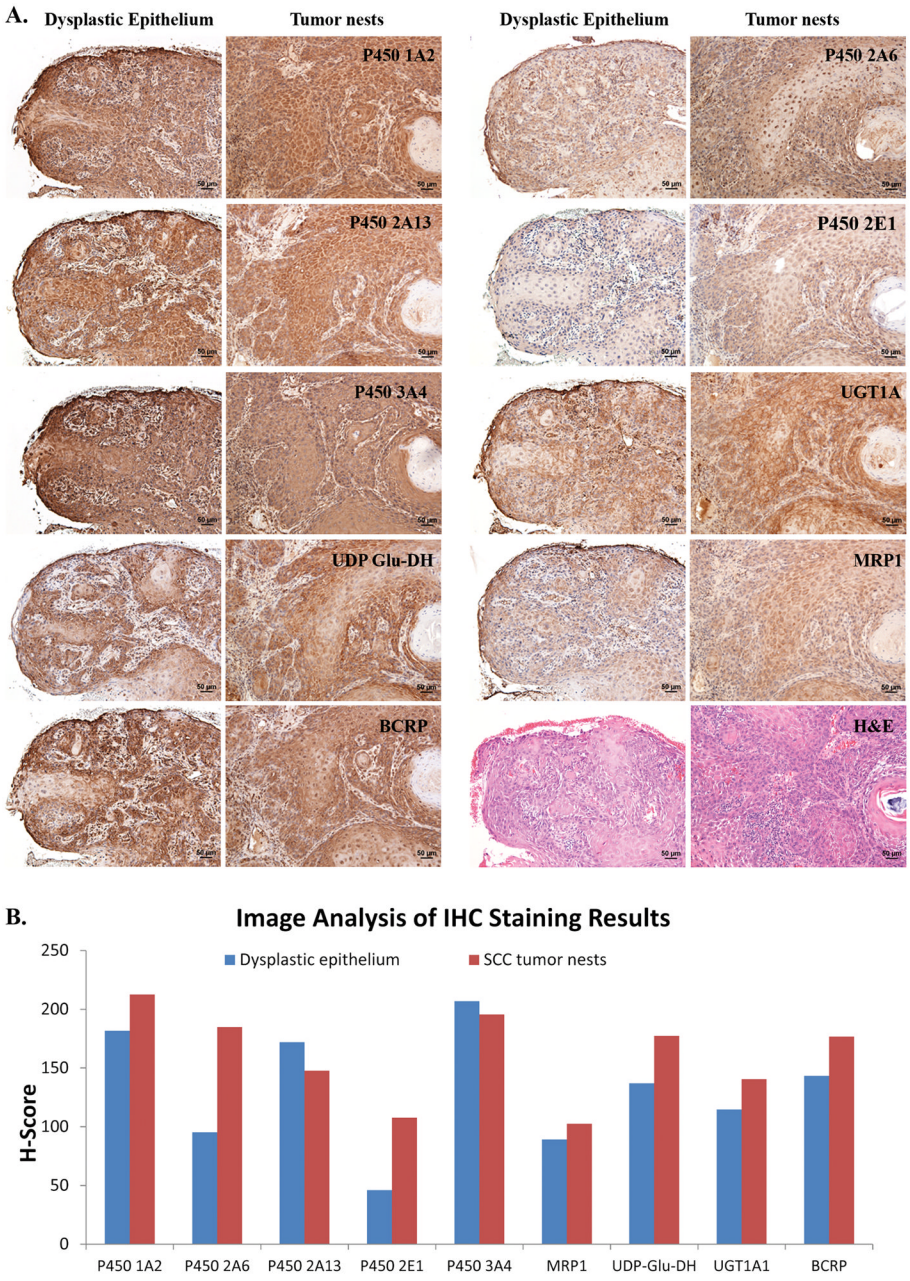

Figure 2.

Fig. 2A portrays a series of immunohistochemical stained images of both the dysplastic surface epithelium (10x image scale) and associated invasive OSCC tumor nests (10x image scale). Notably, both the dysplastic epithelium and tumor nests express all P450 enzymes associated with tobacco-associated nitrosamine metabolism i.e. P450s 1A2, 2A13, 3A4, 2A6, and 2E1. In addition all tissues express UGT1A family, UDP Glucuronide Dehydrogenase, and the Phase III egress enzymes MRP1 and BCRP. Overall, more intense staining is observed in the OSCC tumor nest slides. Levels of P4502E1 and MRP1 are relatively lower than the other metabolic enzymes depicted, with higher relative levels of all enzymes observed in OSCC tumor tissue. Fig. 2B presents the corresponding image-analysis compiled data that depict staining intensity of the metabolic enzymes in overlying dysplastic

epithelia and OSCC tumor tissues. As can also be appreciated in Fig. 2A. OSCC tumor tissue stains most intensely for the majority of metabolic enzymes with the exception of P450s 3A4 and 2A13. Notably, P450 3A4 is a multipurpose metabolic enzyme due to its flexibility and distension while P4502A13 functions primarily to activate NNK.

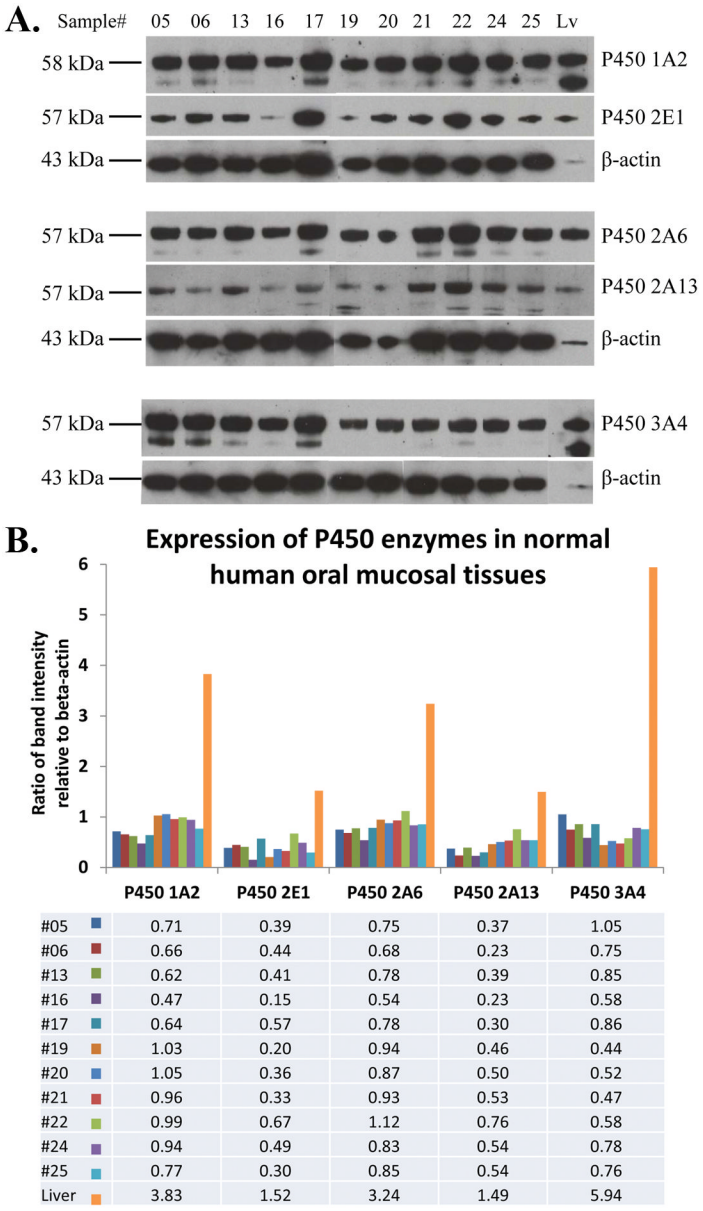

	P450 1A2	P450 2E1	P450 2A6	P450 2A13	P450 3A4
#05	0.71	0.39	0.75	0.37	1.05
#06	0.66	0.44	0.68	0.23	0.75
#13	0.62	0.41	0.78	0.39	0.85
#16	0.47	0.15	0.54	0.23	0.58
#17	0.64	0.57	0.78	0.30	0.86
#19	1.03	0.20	0.94	0.46	0.44
#20	1.05	0.36	0.87	0.50	0.52
#21	0.96	0.33	0.93	0.53	0.47
#22	0.99	0.67	1.12	0.76	0.58
#24	0.94	0.49	0.83	0.54	0.78
#25	0.77	0.30	0.85	0.54	0.76
Liver	3.83	1.52	3.24	1.49	5.94

Figure 3.

Fig. 3A. Immunoblot analyses confirm the presence of all tobacco-associated nitrosamine metabolizing P450 enzyme proteins in normal human oral mucosa. As a positive control, human liver homogenates were included. Fig. 3B. The histogram and accompanying Table (relative protein levels i.e. band density ratios of individual enzyme versus β-actin) depict relative P450 enzyme levels as normalized to the loading control β-actin and quantified by densitometry analysis. There is an approximate 2 fold inter-donor difference in enzyme levels for every P450 analyzed. Also, relative to human liver, oral mucosal P450 levels are appreciably lower.

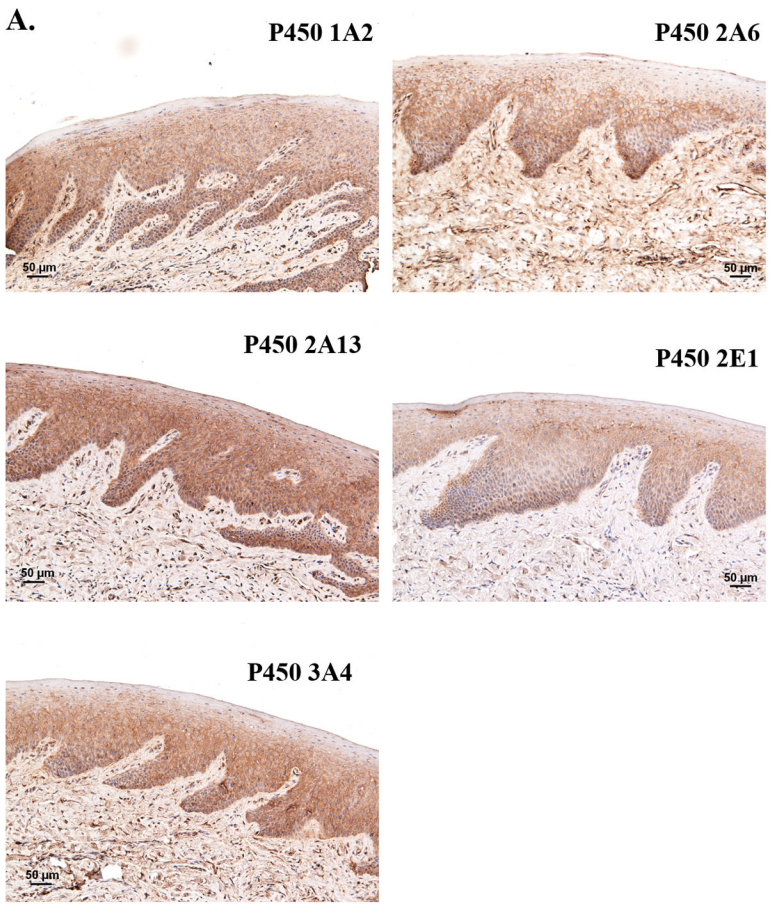

Figure 4.

Depicted in Fig. 4A are representative IHC images (10x image scale) of specimen #06 which show that the localization site for nitrosamine metabolizing P450s is the surface epithelium. As shown by the staining distribution, P450 enzymes are located in the cytosolic-located microsomes of the basal layer keratinocytes and extend into the spinous layers. Similar staining patterns were observed for the other normal oral mucosal specimens. Fig. 4B depicts compiled image analyses data for the normal oral mucosal tissue shown above. Corresponding to the IHC images shown in Fig. 4A the greatest staining intensity was observed in the basilar third of the epithelia and the least intense in the overlying superficial third of the epithelia.

Table I

Distribution and Cellular Localization of Enzymes Responsible for Nitrosamine Metabolism in the Smokeless Tobacco-Associated Squamous Cell Carcinoma Tumor Tissue[a].

Metabolic Enzyme	Potential Carcinogenic or Protective Mechanisms	Enzyme Distribution Profile by IHC-Tumor Tissue
P450 1A2	P450-mediated oxidation of NNK and NNN generates reactive nucleophiles that can mutate and initiate miscoding of DNA. Higher oxidation rates for NNK.	Full thickness surface of dysplastic epithelium, entire tumor islands (100% tumor staining-cytosol staining)
P450 2E1	Inducible by alcohol, oxidative bioactivation of NDMA and NNN to genotoxic products. Highest P450-mediated bioactivation profile for NNN.	Faint staining of dysplastic epithelium, tumor islands (no staining in keratin pearls).
P450 2A6	Enzyme responsible for mutagenic bioactivation of all tobacco-related N-nitrosamines. Genetic polymorphisms observed. Reduced function variants are associated with decreased lung cancer.	Strong cytosolic staining at basilar and suprabasilar cell layers in overlying dysplastic epithelia. Many OSCC tumor islands very intense staining, absence of staining in keratin pearls. Dysplastic and tumor staining intensity is greater relative to normal oral epithelia.
P450 2A13	Strong oxidative bioactivation of tobacco-specific NNK to genotoxic products.	Portions of dysplastic epithelium, tumor nests, 30% shows staining of basal and spinous epithelial layers, central tumor nests.
P450 3A4	Oxidative bioactivation of NNN to genotoxic products	Basal extending into superficial spinous layers of dysplastic epithelium, tumor nests(no staining in central keratin pearls).
UGT 1A Family	Glucuronide attachment enhances water solubility which facilitates urinary excretion	Transition in staining from negligible at dysplastic epithelium to intense at site of invasion, tumor islands (no staining in keratin pearls).
UDP-Glu-DH	Generates UGTs' cofactor, glurcuronide, via oxidation of UDP-glucose	Faint staining in basal and spinous layers of dysplastic epithelium that intensifies at the site of tumor invasion, tumor islands (no staining in keratin pearls).
MRP1	ATP-dependent efflux transporter that participates in the efflux of glucuronidated compounds	Faint staining in dysplastic epithelium that disappears at the site of invasion. Faint to moderate staining in tumor islands (no staining in keratin pearls).
BCRP	ATP-dependent efflux transporter that participates in the efflux of phase II enzyme conjugates	Faint staining in basal and spinous layers of dysplastic epithelium that intensifies at the site of tumor invasion, tumor islands (no staining in keratin pearls).

[a]Immunohistochemical stains were conducted to determine the presence and delineate intracellular localization of these smokeless tobacco relevant metabolic enzymes in OSCC tumor tissue and overlying dysplastic surface epithelia.

Table II

Distribution and Cellular Localization of Enzymes Responsible for Nitrosamine Metabolism in Human Normal Oral Mucosa

Metabolic Enzyme	Western Blot Data[a] (n=11)	Enzyme Distribution Profile by IHC-Normal Oral Mucosa (n=7)
P450 1A2	11/11, 2.2 fold (0.47–1.05)	Intense staining of the basal and spinous epithelial layers.
P450 2E1	11/11, 4.5 fold (0.15–0.67)	Mild to moderate staining of the basal and peribasilar layers.
P450 2A6	11/11, 2.1 fold (0.54–1.12)	Moderate to intense staining observed in basal and spinous layers.
P450 2A13	11/11, 3.3 fold (0.23–0.76)	Intense staining of the basal layer and moderate staining of spinous epithelial layer.
P450 3A4	11/11, 2.4 fold (0.44–1.05)	Intense staining of basal and lower/middle spinous epithelial layers.
UGT 1A, MRP1, BCRP[b]	*These data have been previously reported (11). Notably, all oral mucosal specimens contained all three proteins as demonstrated by Western immunoblotting. IHC staining confirmed an intraepithelial localization.*	

[a] The Western blot data are presented as the number of tissues that demonstrate presence of the specific protein; the fold-difference between the highest and lowest normalized protein levels among the 11 tissues; and the ratio range of respective protein level relative to the housekeeping protein, β-actin.

[b] UGT1A increases water solubility and excretion by glucuronide attachment; MRP1 and BCRP are both ATP–dependent efflux transporters that function to remove Phase II enzyme conjugates such as glucuronides. Our reported study demonstrated expression of these enzymes in 11 human oral mucosal tissues by both Western Blot and IHC staining (11).

Cancer Prev Res (Phila). Author manuscript; available in PMC 2015 January 01.